Petroleum Science 19 (2022) 1779–1792

Contents lists available at ScienceDirect

Petroleum Science

journal homepage: www.keaipublishing.com/en/journals/petroleum-science

Original Paper

Effects of modified graphene oxide (GO) nanofluid on wettability and IFT changes: Experimental study for EOR applications

Ehsan Jafarbeigi [a], Farhad Salimi [a, *], Ehsan Kamari [b, **], Mohsen Mansouri [c]

[a] Department of Chemical Engineering, Kermanshah Branch, Islamic Azad University, Kermanshah, Iran
[b] Department of Petroleum Engineering, Research Institute of Petroleum Industry, Tehran, Iran
[c] Department of Chemical Engineering, Ilam University, Ilam, Iran

ARTICLE INFO

Article history:
Received 25 September 2021
Received in revised form
28 November 2021
Accepted 16 December 2021
Available online 20 December 2021

Edited by Yan-Hua Sun

Keywords:
Wettability alteration
Graphene oxide
Contact angle
Interfacial tension
Zeta potential

ABSTRACT

The application of nanoparticles (NPs) in enhanced oil recovery (EOR) offers a practical approach to resolving some surface-related problems encountered in contemporary technological processes. In this study, graphene oxide nanosheets (GONs) were synthesized by Hummer's method and, then, were subjected to surface modification by hexamethyldisilazane (HMDS) and diazonium sulfonic (DS) compounds. The new combination was known as GO-Su-HMDS. The potential stability of GO-Su-HMDS nanofluids (NFs) was investigated using the zeta (ζ) potential test. A comparative study of the effect of the synthesized NFs on wettability alteration of the reservoir rock was performed using interfacial tension (IFT) and contact angle experiments. According to the results of this study, the contact angle decreased from the initial value of 161° (oil wet) to 35° (water wet). In addition, IFT decreased from 18.45 mN/m for deionized (DI) water to 8.8 mN/m for 500 ppm GO-Su-HMDS NF. Moreover, the results of flooding experiments showed that the NPs of a GO-Su-HMDS concentration of 400 and 500 ppm could increase the oil recovery by 20% and 19%, respectively. The experimental results showed that GO-Su-HMDS NFs with a concentration of 500 ppm have the best efficiency in terms of altering the wettability of the rock from oil wet to water wet. Thus, it can be said that this nanofluid can reduce the contact angle and IFT and also increase the sweeping efficiency of oil.

1. Introduction

The application of nanotechnology in EOR can be possible using two methods: nanofluids (NFs) and nanoemulsions. NFs are defined as nanoparticles with an average particle size of fewer than 100 nm, which can be dispersed in a base-fluid, i.e. distilled water and saltwater (Das et al., 2007, 2021; Taylor et al., 2013; Bhuiyan et al., 2015; Sun et al., 2017; Qi et al., 2018). The EOR in carbonate reservoirs is of great importance due to the existence of large oil resources in them. Besides, chemical enhanced oil recovery (CEOR) methods are used to solve the problem of oil recovery in these reservoirs (Wasan and Nikolov, 2003; Giraldo et al., 2013; Alizadeh-Pahlavan et al., 2018; Kumar and Sharma, 2018). Due to the oil-wetting conditions, carbonate rocks always have a large amount of residual oil in the reservoir, which cannot be produced using conventional primary and secondary recovery methods. In this regard, the use of NPs as one of the third methods can put the amount of oil remaining in the reservoir in the production circuit and is known as a good candidate in EOR processes. Recently, in carbonate reservoirs the use of NPs to enhanced oil recovery (EOR) has been considered by many researchers throughout the oil and gas industry. Carbonate reservoirs, unlike sandstone reservoirs, naturally have either neutral or preferably oil wet state, and therefore, the recovery of oil with waterflooding methods is relatively low and inefficient. Therefore, the wettability of carbonate rock with addition of chemical agents can be improved and increases the effectiveness of the waterflooding process. The role of NPs and their performance in the field of recovery of oil from reservoirs due to their attractive features has been prominent in the past by many researchers. However, choosing suitable NPs and applying it in carbonate reservoirs is not just the limiting factor to guarantee better performance in EOR, but on the other hand, they depend on the stability and their dispersion in water conditions (Gomari et al., 2019; Taleb et al., 2021). Nearly 60%–70% of world's oil is trapped in carbonate reservoirs (Allan and Sun, 2003; Ranka

* Corresponding author.
** Corresponding author.
E-mail addresses: f.salimi@iauksh.ac.ir (F. Salimi), kamarie@ripi.ir (E. Kamari).

https://doi.org/10.1016/j.petsci.2021.12.022

et al., 2015; Cheraghian and Hendraningrat, 2016; Jafarbeigi et al., 2020; Ghasemi et al., 2020; Nowrouzi et al., 2020a). The main challenge of nanoparticle-based EOR (nano-EOR) in carbonate reservoirs is to maintain the average particle size and enhance colloidal stability of NFs (Ji et al., 2011; Abbasabadi et al., 2016; Hendraningrat and Torsæter, 2016; Zhang et al., 2016 Nowrouzi et al., 2020b). The most important factors affecting the adequate performance of NFs in the porous media are the wettability alteration (WA) and interfacial tension (IFT) (AfzaliTabar et al., 2017; Bagherpour et al., 2019; Hamouda and Murzin, 2019; Ahmadi and Shadizadeh, 2013; Ayirala et al., 2020; Belyaeva and Schneider, 2020; Esmaeilzadeh et al., 2020; Fenter et al., 2020; Shakiba et al., 2020). In this regard, WA techniques such as low-salinity water flooding, surfactant flooding, and thermal stimulation can enhance the recovery and improve sweep efficiency (Abu-Al-Saud et al., 2020; Saeb et al., 2020; Guo et al., 2020; Yao et al., 2022). Recently, NFs have been widely studied in the oil and gas industry, especially in EOR. In this sense, nano-liquids can release oil from the porous media by altering the wettability of the rock (Fletcher and Davis, 2010; Suleimanov et al., 2011; Cocuzza et al., 2012; Al-Anssari et al., 2016; Cheng et al., 2017; Abdo-Saleh and Al-Hammadi, 2018; Abhishek et al., 2018; Hamouda and Abhishe, 2019; Ahmadi et al., 2020), reducing the IFT between the injected fluid and the oil (Alomair et al., 2014), as well as the spontaneous formation of the emulsion (Mensah et al., 2013) and somehow affecting the EOR. In the presence of silica NPs, Hendraningrat et al. (2013) investigated the effect of WA mechanism using contact angle measurement. Roustaei et al. (2013) studied the effect of nanoparticle concentration on IFT and water-wet in their experiments, which included injecting NFs into the core containing 5 wt% of salt (NaCl). The results of these studies showed that by increasing the concentration of silica NPs from 1 wt% to 4 wt%, in addition to changing wettability, the IFT reduces from 25 to 5 mN/m. Yao et al. (2021) conducted a lecture review on carbonate rock wettability and EOR using surfactants. They presented techniques to evaluate the effect of wettability alteration. This study discusses strategies related to the cost of surfactant, surface adsorption and challenges at high temperature, conditions of high salinity reservoirs. Also, some obscure issues existed in this regard. In different systems, surfactants such as single surfactants and a mixture of surfactants have been effective in achieving the process of changing the wettability of rock. On the other hand, the results showed that the Gemini surfactants have many desirable properties, which need to be investigated further about the understanding of its mechanisms and the performance of changing wettability. In another study, Zheng et al. (2017) reduced the IFT and WA of the rock by dispersing SiO_2 NPs in polyethylene glycol. In this regard, an incremental oil recovery of 17% was achieved using the combined effect of these materials in their study. Furthermore, Yin et al. (2019) enhanced the oil recovery by 18% at a concentration of 0.005 wt% and by placing silica (SiO_2) over janus graphene oxide (J-GO). Examining the compatibility between the ζ-potential process with salinity as well as core-scale experiments, Mahani et al. (2015, 2017) showed that the combination of surface charge alteration with the expansion of the electric-double-layer (EDL) could be used as a recognizing an acceptable mechanism for altering wettability in carbonate rocks. In the present work, the synthesis and functionalization of graphene oxide nanosheets (GONs) have been studied in order to prepare a new chemical for altering the wettability and enhancing oil recovery. In previous studies, limited experiments have been performed on the effect of surface modification of this material on EOR. Moreover, only a limited number of experiments have been performed on the effect of surface modification of this material on EOR and less attention has been paid to the comparison of wettability mechanisms. In this regard, by synthesizing and functionalizing the N-doped graphene, Rezaei-Namin et al. (2019) altered the wettability of the sandstone core from oil wet to water wet at 500 ppm concentration and also reduced the CA from the reference value of 128° to 68.3°. On the other hand, they increased the oil recovery by 16.16%. Furthermore, Afzali Tabar et al. (2017) determined the best nanohybrids that can be used as a pickering emulsion for EOR. They prepared nanohybrids at concentrations of 10% N-GQDs/MQDs and 50% N-GQDs/MQDs nanohybrids and, then, reduced the CA for these two types of nano-hybrids from the reference value of 87.73° to 64.57° and 69.47° respectively. Therefore, in this new work, the GO functionalized by HMDS and diazonium sulfonic (DS) compounds indicate a better performance due to the functional groups placed on the structure, as compared to previous studies. The synthesized GO-Su-HMDS NFs was subjected to experiments involving IFT and CA. As was already mentioned, the present study aimed at altering the wettability of reservoir rock and increasing the water wet condition of rock in the presence of GO-Su-HMDS NFs to increase oil production. On the other hand, this leads to the sound formation of a wedge film due to structural disjoining pressure. This wedge film results in adsorbing the water on the rock surface and, thus, increasing the sweep efficiency of oil recovery. Herein, CA, NF stability evaluation, ζ-potential, IFT, adsorption test and viscosity measurements were performed to investigate the physical properties of the GO-Su-HMDS. Core-flooding experiments were performed to test the effect of the GO-Su-HMDS NF when used for EOR. The synthesized GO-Su-HMDS NF was analyzed and investigated using Fourier transform-infrared spectroscopy (FT-IR), X-ray diffraction (XRD), and field emission-scanning electron microscopy (FE-SEM) analysis. The synthesis and application of these new findings make it possible to examine the effect of nanoparticle concentration parameters on the selection of suitable NPs for EOR.

2. Experimental

The experimental procedures included GO-Su-HMDS synthesis and characterization of GO-Su-HMDS nanoparticles are described in Fig. 1. Moreover, the static experimental part consists of the preparation and stability observation of GO-Su-HMDS NFs and their effects on IFT reduction, CA tests, adsorption tests and, finally, core-flooding experiments, which are explained in detail below.

2.1. Experimental materials

Graphite powder (99.8% purity) was provided by Sigma Aldrich and other reagents used in this study were all supplied by Merck. All reagents were of analytical grade and were used as received without further purification.

2.2. GO-Su-HMDS synthesis process

In this research, GO was synthesized using Hummer's method. The Hummer's synthesis process, which was carried out by Zhu et al. (2010) as well as Marcano et al. (2010), is summarized as follows: First, 50 mL of sulfuric acid (H_2SO_4, 98%) was mixed with 1 g of graphite powder (99.8% purity) and, then, stirred for 10 min. Afterwards, 7 g of potassium permanganate ($KMnO_4$, 99.9% purity) was added to the mixture for 10 min. The mixture was then stirred at 45 °C for 24 h to complete the reaction. Subsequently, 160 mL of water was added to the mixture. After 20 min, 55 mL of hydrogen peroxide (H_2O_2, 30% purity) was also added. The mixture was then centrifuged and washed with HCl (10%) several times. Deionized (DI) water was used to wash the mixture until it reached neutral pH. Finally, 500 mL of DI water was added to the mixture and then exposed to sonication. The mixture was then centrifuged to

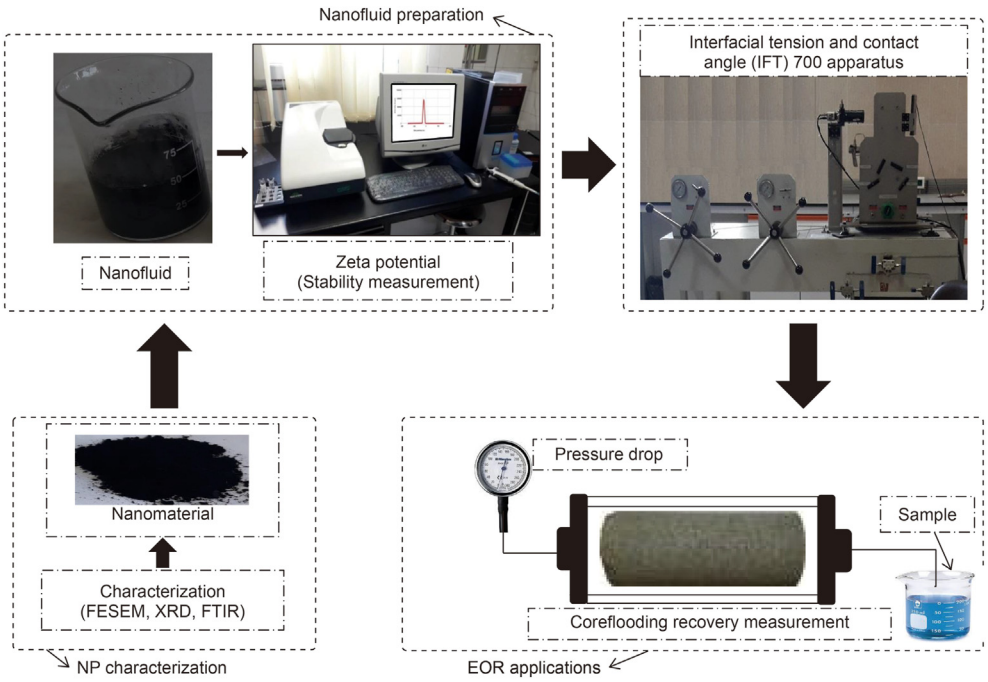

Fig. 1. Schematic representation of the experimental procedures for synthesizing GO-Su-HMDS nanoparticle and its application.

separate the unstable part from the stable part. In the end, the uniformed graphene oxide (GO) particles were obtained in water.

Fig. 2 shows the step-by-step synthesis and preparation of nano-graphene oxide (NGO). In the following, GO-DS synthesis is discussed. More information about the process of GO, functionalization by DS, can be found in the research by Peng et al. (2013). In this work, to synthesize GO-DS, 4-sulfo-benzene diazonium salt must first be synthesized and is synthesis procedure is described as follows. A total of 6.2 g of 4-amino-benzene sulfonic acid was dissolved in water and, then 29 mL of HCl (20%) was also

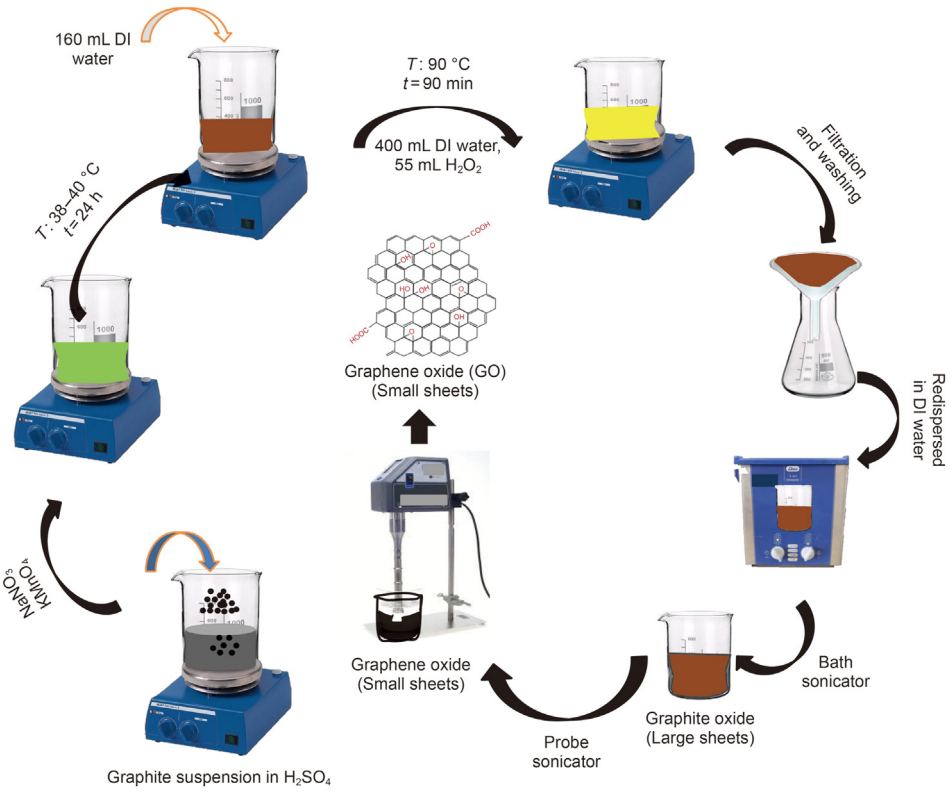

Fig. 2. Step-by-step schematic view of nanoparticle synthesis GO.

added to the solution. Afterwards, 2.5 g of sodium nitrite was solved in 15 mL of water. After stirring for another 1 h at 0–5 °C, the white precipitate of 4-sulfo-benzene diazonium salt was formed. On the other hand, 2 g of NGO was added to 200 mL of water for (graphene oxide-diazonium sulfonic) synthesis and, then, 1.2 g of sodium dodecylbenzene sulfonate (SDBS) was added to the solution to complete the (graphene oxide-diazonium sulfonic) synthesis process. Subsequently, an hour after stirring, 2 g of 4-sulfo-benzene-diazonium salt solution was added slowly to the GO dispersion under mild stirring, and, consequently, GO-DS was synthesized. In the next step, the synthesis of GO-Su-HMDS NPs was investigated. To synthesize GO-Su-HMDS NFs, GO-DS NPs must be functionalized. In this experimental survey, to functionalize GO-DS, hydroxyl (OH) groups were first replaced with chlorine using thionyl chloride in order to functionalize GO-DS and, then, stirred under reflux conditions. In the following, the excess amount of thionyl chloride was separated via the distillation method. Thereupon, the solid was mixed with 12 mL of HMDS and 45 mL of dichloromethane (CH_2Cl_2) and then washed with ethanol (C_2H_6O) and water after centrifugation. In the following, the product was dried in the oven. Moreover, 0.7 g of this substance was spread in 45 mL of CH_2Cl_2 to complete the reaction. Subsequently, the functionalized GO suspension was centrifuged, washed with C_2H_6O and H_2O several times, and dried the sample in the oven at 60 °C. Finally, GO-Su-

HMDS was reached as the final product. The steps of GO-Su-HMDS synthesis are shown in Fig. 3.

The properties of the synthesized GO-Su-HMDS NPs, such as morphology, the texture of the system, its surface and the presence of its functional groups on it were obtained by FT-IR, XRD (Rigaku Ultima IV) and FE-SEM (Model Mira 3) analyses.

2.3. Carbonate samples

The type of reservoir rock used in this research is carbonate reservoir rock. Thus, the characteristics of the cores are shown in Table 1. The core plugs were cleaned in the Soxhlet device using different solvents. Crude oil used, which was taken from one of the Iranian western carbonate reservoirs, had a density of 0.833 g/cm^3 and a viscosity of 16.31 cP, respectively. The FE-SEM equipped energy dispersive X-ray spectroscopy (EDS) analysis is applied to identify the carbonate minerals. In this regard, the elements present in carbonate rock are shown in Fig. 4.

Table 1
Dimensions and properties of the core plugs.

Core No.	Core length, cm	Core diameter, cm	Porosity, %	Permeability, mD
Core 1	5.105	3.799	17.491	0.262
Core 2	5.110	3.800	22.613	0.483

2.4. Methods

2.4.1. Emulsion preparation

The amphiphilic nature of the functionalized graphene oxide (called GO-Su-HMDS) was investigated by preparing oil in water emulsions. Accordingly, the amount of 7 mL of toluene was added to 7 mL of the NF, separately dispersed at specific concentrations (200, 300, 400 and 500 ppm). Next, the vials containing organic-phase and aqueous-phase were placed in an ice bath for 15 min (Radnia et al., 2018). These mixtures were then subjected to homogenization for 35 s using a probe sonicator; so that, in the process of homogenizing the mixtures by sonication, the vials were still kept in an ice bath to prevent temperature rise during the sonication process. After 24 h of sample preparation, light micrographs were taken from the prepared emulsions on glass slides using a BM2000 microscope (ECLIPSE LV100POL, Nikon, Japan). The diameter of the emulsion droplets was measured through Digimizer software.

2.4.2. Contact angle and interfacial tension measurements

The carbonate core plugs were immersed in crude oil for 21 days at 120 °C to become the initial oil wet state. After aging the

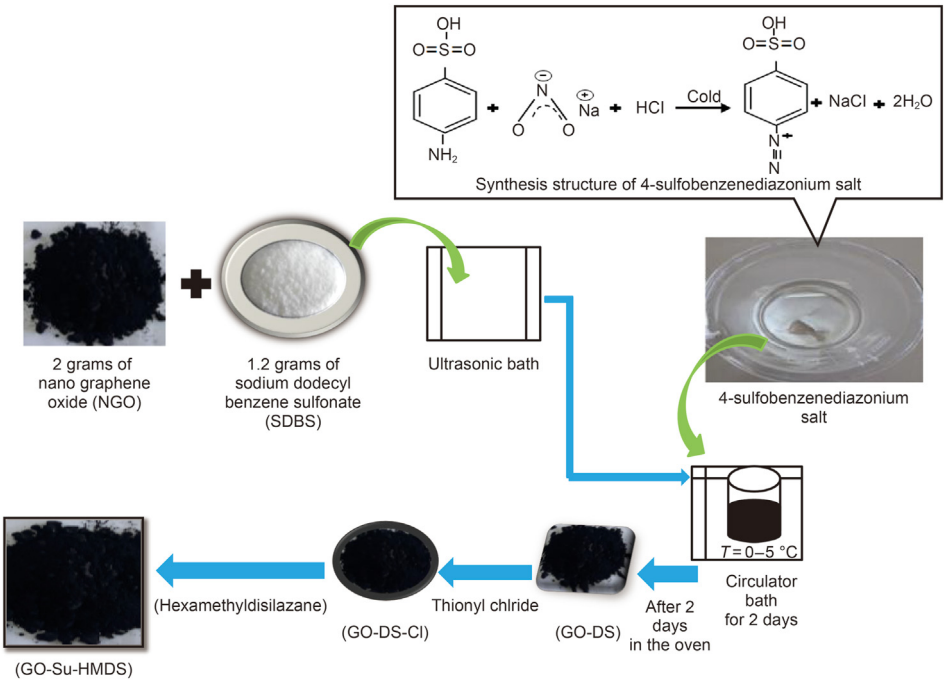

Fig. 3. Step-by-step schematic view of nanoparticle synthesis GO-Su-HMDS.

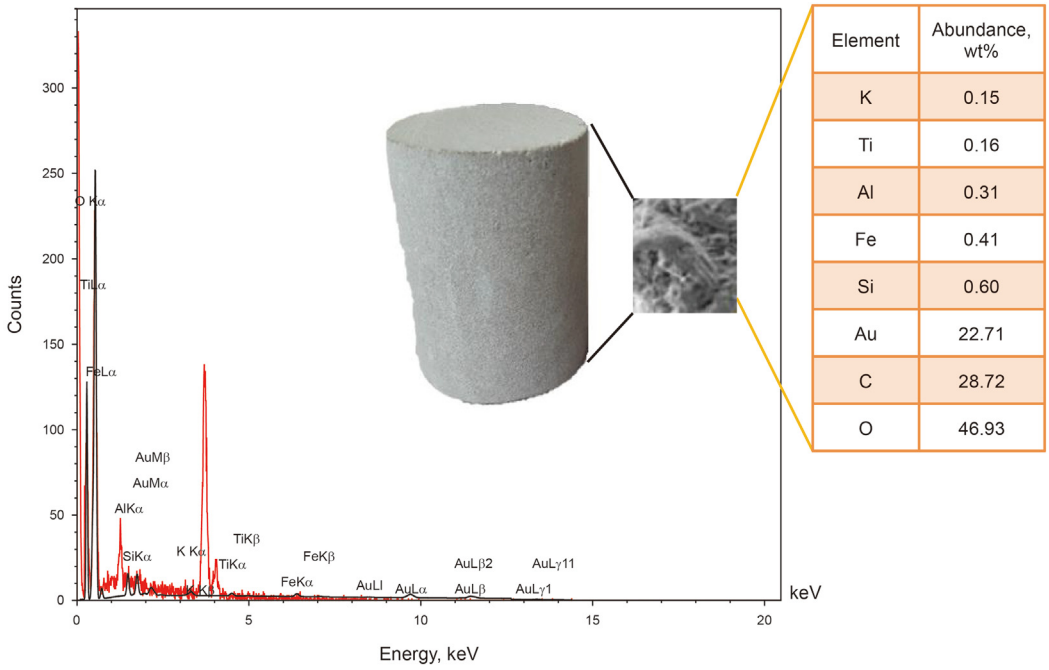

Fig. 4. FE-SEM/EDS image of the prepared carbonate sample.

carbonate cuts in the NF, the WA in rock was evaluated using an interfacial tension meter, IFT 700 (Vinci Technologies, France).

The CA is the most direct parameter to indicate the wettability of a solid surface (Wei and Babadagli, 2018). The wettability degree of the surface is defined according to the CA in the three-phase system (water-oil-rock) interface, i.e. the CA range for the strong water wet condition is 0°–30°, the relatively water wet condition is 30°–90°, neutral or intermediate is 90°, the relative oil wet is (90°–150°) and the strong oil wet condition is in the range of 150°–180° (Anderson, 1986a, 1986b; Rostami et al., 2019).

IFT measurement of crude oil and NFs were also performed under ambient conditions using a sessile drop method. A syringe with a specific diameter and U-shaped needle was embedded to measure IFT so that the needle was in contact with the crude oil. Besides, an optical vessel was completely filled with NF. The concentration of NFs was between 200, 300, 400, and 500 ppm. In the vessel, the tip of the "u-shaped-needle" was placed and, then, the drop of crude oil was positioned on the tip of the needle. The image of the drop was recorded using a CCD or photographic device with macro lenses. Afterwards, the image of the dropper was analyzed using the Image J software. Finally, the IFT value was determined.

2.4.3. Adsorption experiments

The static adsorption method was used to investigate the adsorption behaviour of rock in the presence of GO-Su-HMDS NPs. The measurement was performed at room temperature. Herein, the cores were first cleaned and then crushed. The crushed cores were used as the raw material for the adsorbent. In the next step, the adsorbent was sieved by a set of standard sieves, which had a range of 70–200 μm. Then, after 12 h, the mixed samples were precipitated. At the end of the steps, the residual concentration of NF was 279 nm, which was obtained using a UV–Vis-spectrophotometer. The wavelength of maximum absorbance, which belonged to GO-Su-HMDS NF, was then measured (Dehghan-Monfared et al., 2015; Abhishek et al., 2018). Finally, the equilibrium concentration and the initial concentration of GO-Su-HMDS and the initial volume (V) of the NF and the mass (m) of the rock can be used to calculate the adsorption capacity of GO-Su-HMDS on rock using Eq. (1).

$$q = \frac{V(C_0 - C_e)}{m} \quad (1)$$

where q is the adsorption capacity, mg/g; C_0 is the initial concentration of GO-Su-HMDS, mg/g; C_e is the equilibrium concentration of GO-Su-HMDS, mg/g; V is the NF initial volume, mL; m is the carbonate rock mass, g.

2.4.4. Coreflood system

The GO-Su-HMDS NF flooding operations were performed to enhance the oil production process and identify its impressive applications in oil reservoirs. The flooding process was performed in the core at room temperature. During the flooding operation, the injection process of DI water and GO-Su-HMDS NF was performed at a rate of 0.2 mL/min and 2 PV. Therefore, the GO-Su-HMDS NF flooding process to the core began when the oil production process was significantly reduced during the water-flooding process. Accordingly, the injection process into the core continued until about 5 PV. In this regard, Fig. 5 shows the general schematic of the core-flooding equipment and devices.

3. Experimental results

3.1. Characterization of functionalized nanoparticle and stability investigation

In the present study, the X-ray diffraction (XRD) pattern of the modified NPs GO is illustrated in Fig. 6. As can be seen from Fig. 6, the structure of GONs has changed from morphine to crystalline, which shows that by functionalizing different groups on the surface of GONs, the distance between the layers increases, and it can be concluded that functional groups are well placed on the surface. Fig. 7a, b shows the FE-SEM image of the modified NPs GO in which the textures are obvious at 10 μm and 200 nm. Moreover, Fig. 7

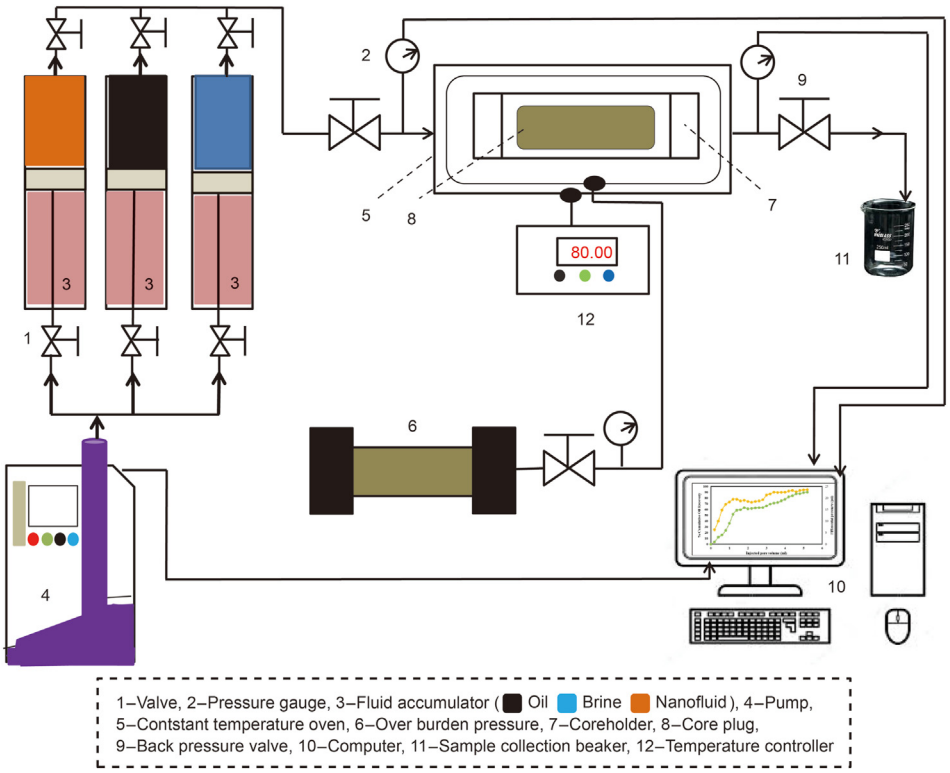

Fig. 5. General schematic of the used flooding system.

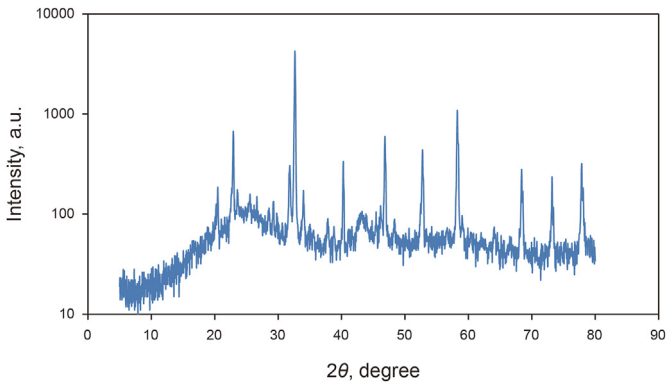

Fig. 6. XRD pattern of GO-Su-HMDS nanoparticles.

confirms the emission of HMDS throughout the GO structure that covers the entire GONs surface. Thus, Fig. 7 clearly shows the morphological FE-SEM image of the GO-Su-HMDS structure. The FT-IR spectra of pristine and the functionalized graphene oxide are shown in Fig. 8. The signal at 2800 cm^{-1} illustrates the "sp^2" character of the nanoparticle (Tuteja et al., 2015). The absorption signals at around 1224.26 and 3387.4 cm^{-1} may be attributed to the "C–O" groups and "O–H" stretching vibrations, respectively. The existing signal in the range of 1618.85 cm^{-1} corresponds to the N–H signal. The sulfonic acid functional groups in the presence of sodium dodecyl benzene sulfonate composition in the GO-DS structure are also shown in Fig. 8, having the following signals at 1008, 1052, and 1121 cm^{-1} (Li et al., 2013; Mondragon et al., 2012). Regarding GO-DS-Cl, the characteristic band at 1618.85 cm^{-1} corresponds to the N–H bending. The appearance of a relatively broadened band in 1404.34 cm^{-1} indicates the C–N bond stretching (Tuteja et al., 2015). In addition, the presence of amine (N–H) groups in the structure of graphene oxide was confirmed by signals from 3005 to 3477.127 cm^{-1}. The peaks at 1157.01 and 1105.01 cm^{-1} confirm the presence of sulfonic (S) acid groups in the GO-Su-HMDS plane (Mondragon et al., 2012). The Si–O signal is also in the range of 1100 cm^{-1} (Ture et al., 2020). Thus, the structure of GO-Su-HMDS NF was demonstrated through the analysis of the FT-IR diagram. As a result, due to its synthetic structure, this NF can show a positive performance in oil recovery. In the following, the stability of NFs was investigated. The stability of spreading the GO-Su-HMDS NFs dispersion at the 500 ppm concentration was investigated; so that, after preparing the NFs, they were transferred to transparent vessels. Furthermore, in order to carry out the process, the change in the stability of their dispersion was controlled over time. NFs has a black schematic appearance. On the contrary, after 37-h of preparing the GO-Su-HMDS NFs, the results of stability analysis of GO-Su-HMDS NF show that this NF is stable for 37 h. This durability during this time is due to the presence of functional groups affecting the structure of GO-Su-HMDS NPs. At 3, 6, and 9 pH values, possible changes occurred in the ζ-potential of GO-Su-HMDS NPs. According to Fig. 8c, the GO-Su-HMDS nanofluid with pH = 9 is in the proximity of −30 mV, which indicates a stable colloidal suspension for NF at this concentration. ζ-potential changes for the GO-Su-HMDS dispersion at different pH values are shown in Fig. 9. Herein, the negative charge at the GO-Su-HMDS level is related to the deionization of the following functional groups: Si and S=O. As the pH increases, the negative charges resulting from the −S groups would also increase. Besides, at baseline pH values, the GO-Su-HMDS surface charge becomes more negative. This led to lowering the ζ-potential values. This suggests that the stability of GO-Su-HMDS spreading is more due to its water wet conditions, which is in fact because of the presence of electrostatic repulsion (Schramm, 1992; Radnia et al., 2017). The more

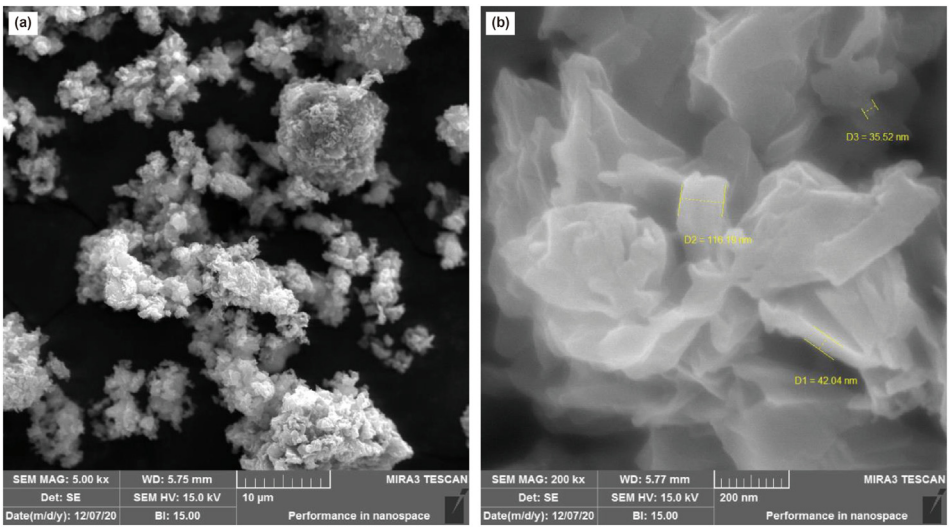

Fig. 7. FE-SEM image of GO-Su-HMDS. (**a**) 10 μm, (**b**) 200 nm.

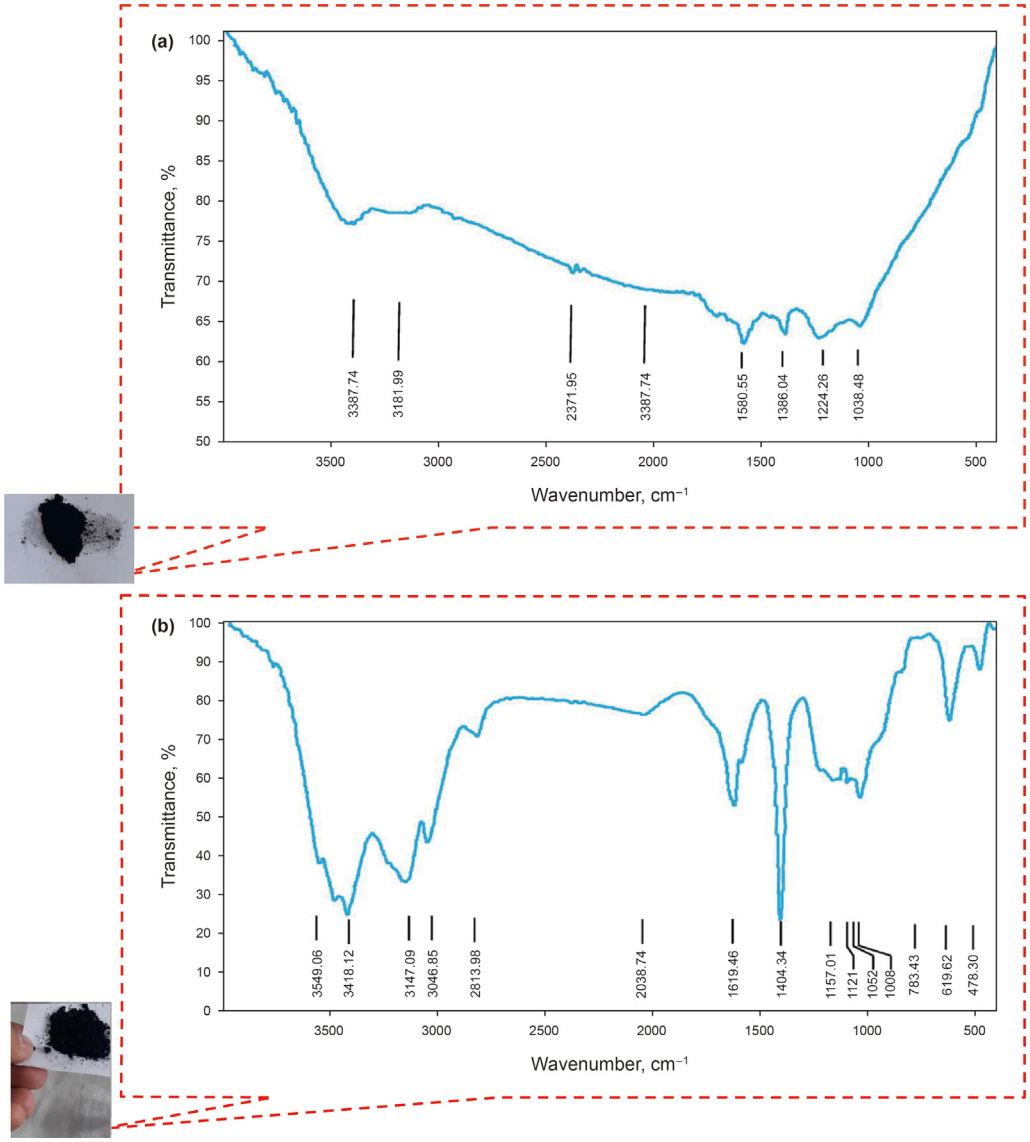

Fig. 8. FT-IR spectra of graphene oxide nanoparticles (GONs) and synthesized nanoparticles namely GO-Su-HMDS.

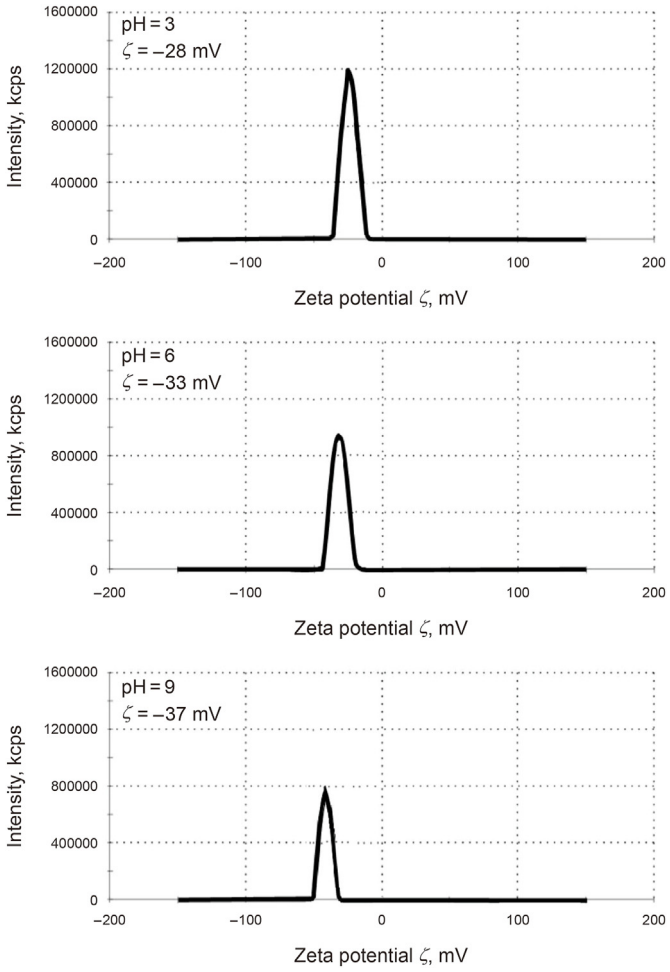

Fig. 9. Changes of ζ-potential for the GO-Su-HMDS nanofluid with different pH values.

negative ζ-potential indicates the greater strength of GO-Su-HMDS NFs to separate hydroxyl (−OH) groups attached to the surface, resulting in increased oil recovery. Regarding what has been mentioned so far, the ability of NFs to alter surface wettability can be effective. As shown in Fig. 10, the concentration effect of the

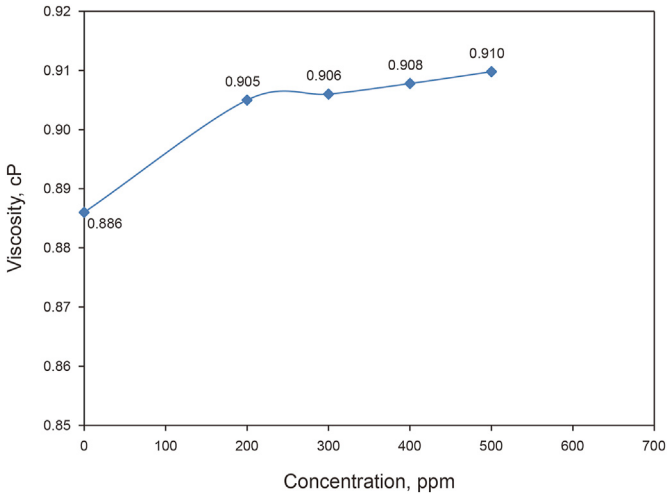

Fig. 10. Viscosity change with concentration for GO-Su-HMDS nanofluids.

synthesized GO-Su-HMDS NPs on the viscosity is somewhat minor, so that the amount of viscosity increased while increasing the concentration of NPs, albeit to a very small extent. In this regard, the viscosity of GO-Su-HMDS NF increased from 0.886 cP for DI water to 0.9050, 0.9060, 0.9078 and 0.9098 cP for concentrations of 200 ppm, 300 ppm, 400 ppm and 500 ppm, respectively. Regarding the industrial applications, such an increase in viscosity is negligible, especially at low GO-Su-HMDS concentrations.

3.2. Amphiphilic nature of GO-Su-HMD and interfacial tension tests

In order to measure GO-Su-HMDS NF emulsion, water and oil emulsion solutions were first prepared at different concentrations and, then the samples were examined. According to the observations, when a drop of emulsion is dispersed in pure water, this emulsion remains as a droplet in pure oil, which is known as toluene. Herein, this state of emulsion is known as an oil/water emulsion. In addition, the results indicate that a small amount of GO-Su-HMDS can form emulsions with an average droplet size of 3.50 μm. The optical micrographs of Pickering emulsions at different concentrations of 200, 300, 400 and 500 ppm were investigated. Our observations show that a drop of emulsion disperses in pure water, while it remains as a drop-in pure oil (here toluene). Therefore, in this case, the emulsion type is inferred to be an oil/water emulsion. The microscopic images and the average droplet diameter of the emulsions are calculated and shown in Fig.11. In this regard, with a decreasing trend, the average droplet size has decreased from 3.50 to 1.18 μm. This trend of decreasing droplet size is due to the increase in GO-Su-HMDS concentration from 200 to 500 ppm. On the other hand, the emulsion's droplet size is considered a function of the amount of IFT. Accordingly, the IFT between oil and NFs was measured to survey the effect of GO-Su-HMDS NF on the IFT properties of oil and water. Like the method described by Radnia et al. (2018), in the present study, IFT was measured. In order to examine the surface properties of oil and water by GO-Su-HMDS NFs, the IFT between oil and GO-Su-HMDS NFs was also investigated at different concentrations. The IFT value of DI water versus crude oil is 18.45 mN/m. This value is used as a reference value in the IFT test for GO-Su-HMDS NFs. Fig. 12 shows the IFT diagram for GO-Su-HMDS NFs and their calculated IFT values at different concentrations. The GO-Su-HMDS NF showed high efficiency in IFT reduction at the (oil-water) interface. The ratio of IFT reduction for the synthesized NFs was 8.8 mN/m of the reference value at 500 ppm. The amount of IFT is sensitive to the concentration of NF; so that, as the concentration of NF increases, the IFT decreases. It is impossible to measure the IFT value at the nanofluid concentrations higher than 500 ppm because both the aqueous and organic phases were dark. Moreover, and the shape of the oil drop cannot be analyzed to obtain the IFT value. Therefore, in this regard, the shape of the oil drop cannot be analyzed to obtain the IFT value. According to the above description, the IFT value for the water phase with GO-Su-HMDS, as shown in Fig. 12, is lower than the IFT value of DI water. In addition, it can be said that water phases can act as a surfactant at the contact line of crude oil and water due to the presence of the surface-active agents. According to the above points, the simultaneous presence of carbon base and Si groups on a single molecule made the GO-Su-HMDS sheets look like active surface agents. Therefore, thermodynamic stability is achieved due to their dependence on each water and organic phase, and their accumulation at the oil and water interface. Herein, this growing trend is known as solid particle surfactants. It is worth mentioning that the formation of Pickering emulsions significantly reduces the amount of the IFT. Fig. 13 illustrates the structures of the amphiphilic nature (a hydrophilic head (polar)

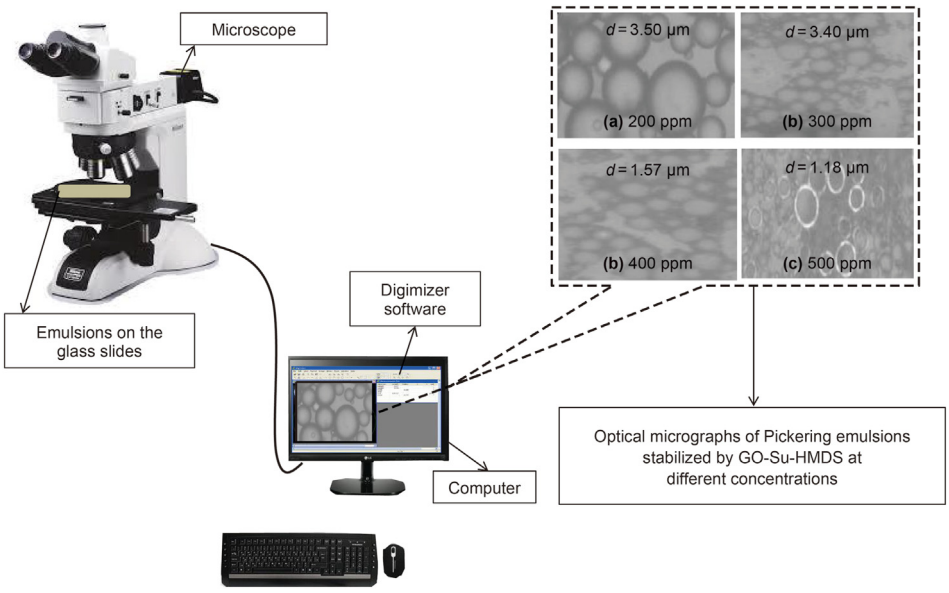

Fig. 11. Forming Pickering emulsions prepared for GO-Su-HMDS nanofluid at different concentrations.

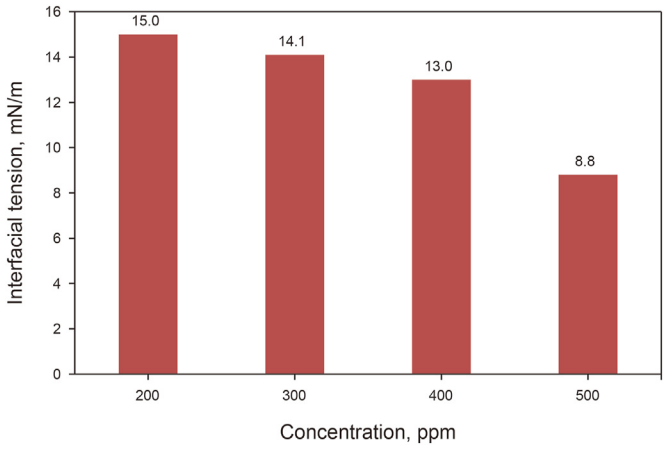

Fig. 12. IFT diagram at different concentrations of GO-Su-HMDS nanofluid.

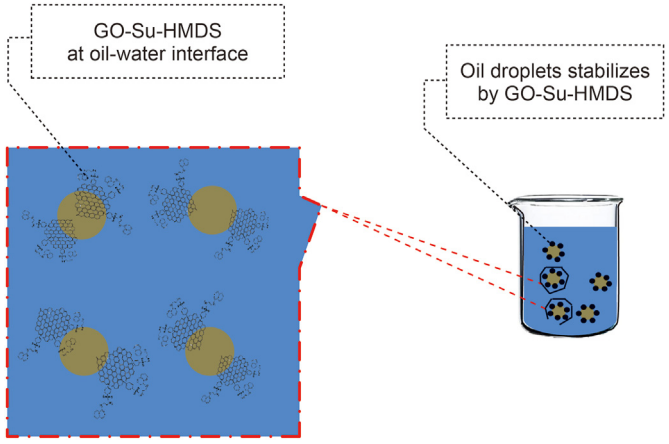

Fig. 13. Schematic representation of amphiphilic GO-Su-HMDS at the crude oil and water contact surface.

and a hydrophobic head (non-polar)) of GO-Su-HMDS sheets at the (oil-water) interface, schematically.

3.3. Wettability alteration of carbonate and adsorption experiments

Herein, the oil-water CA is measured on the carbonate rock surface to assess the WA of carbonate cuts that have been aged at different concentrations of GO-Su-HMDS. The oil CA in the initial conditions for carbonate samples subjected to aging is 161°. Furthermore, the CA of the oil on the surface of the slide or carbonate samples in GO-Su-HMDS solution, with the concentration of 200, 300, 400, and 500 ppm, is about 100°, 83°, 51°, and 35°, respectively, indicating the existence of a strong water wet condition created by GO-Su-HMDS NF to alter the wettability of the carbonate core plug. The schematic of the WA of the NFs versus concentration is shown in Fig. 14. The use of GO-Su-HMDS NF can increase the sweep efficiency of oil due to the presence of effective functional groups on its structure. GO-Su-HMDS NF with a concentration of 500 ppm was selected as the most potent concentration in order to alter the reservoir rock wettability into water wet.

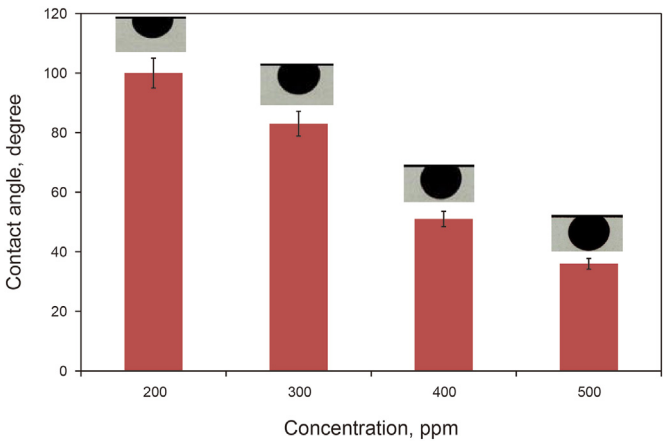

Fig. 14. Changes in the CA of GO-Su-HMDS nanofluids.

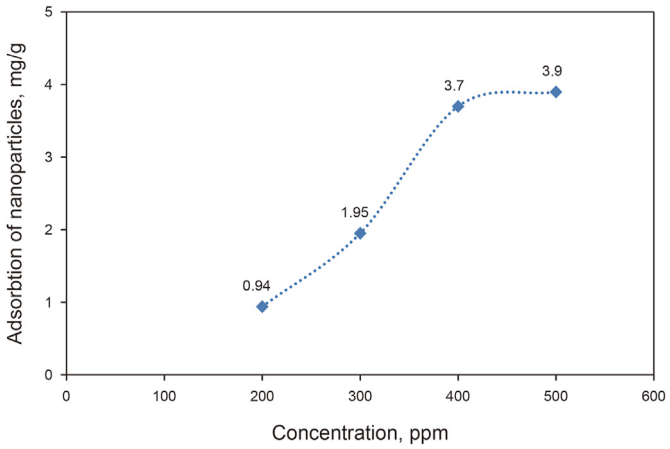

Fig. 15. Adsorption of GO-Su-HMDS on the surface of carbonate rock.

On the other hand, an adsorption test was performed in the presence of rock. Here, this test aims to gain knowledge of the GO-Su-HMDS NF properties to change the properties of rock. According to Fig. 15, the presented results confirm the effectiveness of synthetic NFs in the hydrophilicity of carbonate core rock. Moreover, as indicated in Fig. 15, a certain amount of GO-Su-HMDS NF is adsorbed on the rock surface and, accordingly, the graph shows an increasing trend with a rising GO-Su-HMDS NF concentration.

3.4. Potential implications of proposed theory and findings into practice for high production

In this study, the presence of silicon (Si) and hydroxyl (−OH) groups in the rock structure and also the presence of hydrogen (H), oxygen (O), sulfonic (S) and silicon (Si) groups in the structure of GO-Su-HMDS NPs would indicate the effective use of this NF in altering the rock wettability towards water wet conditions. This can be due to the coordination in the structure of rock and NF and, on the other hand, indicates a very good exchangeability between minerals in the rock and the functional compounds in NF, upon which those trends interact with each other. According to these interpretations, GO-Su-HMDS NF is adsorbed on the rock surface due to structural exchange with the rock, causing a change in the rock wettability and changing the oil wet conditions of the rock to the water wet conditions. This mentioned process leads to the best possible EOR. Thus, when the surface of a rock is well covered with hydrophilic groups, a water film is formed on the rock surface and the oil droplets. Afterwards, the oil droplets are well placed under that film, which causes significant separation of oil from the surface

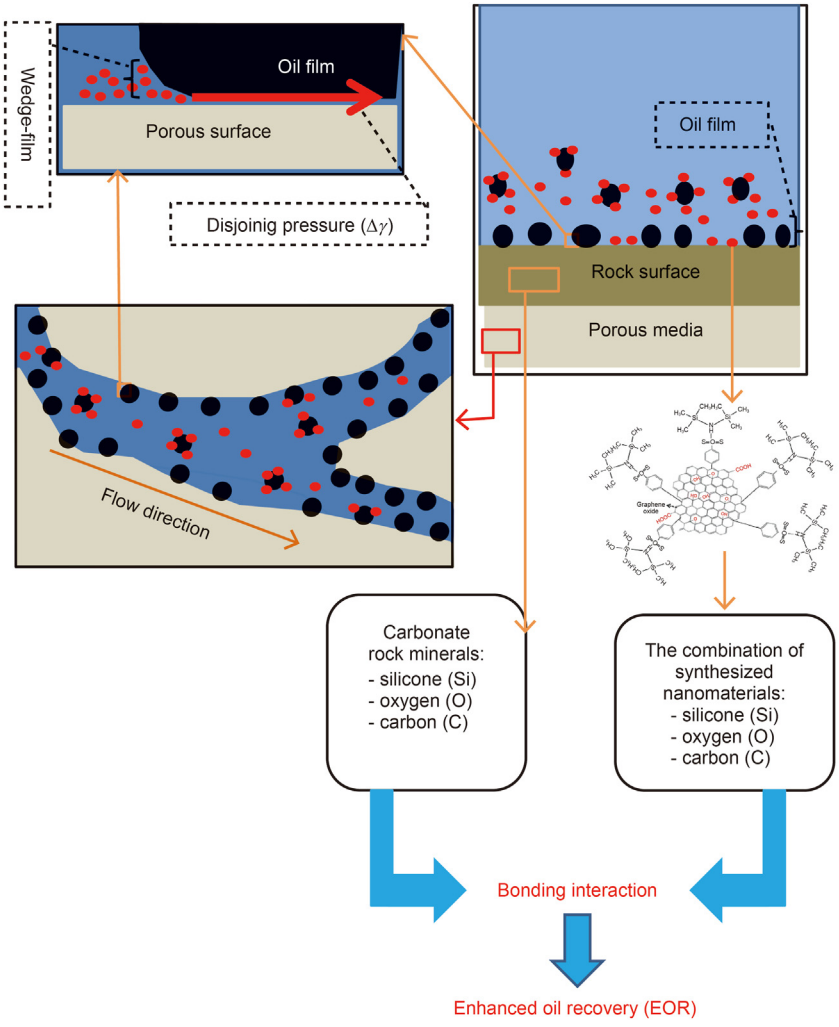

Fig. 16. Mechanism of structural disjoining pressure performance and adsorption of GO-Su-HMDS nanofluid on carbonate rock surface.

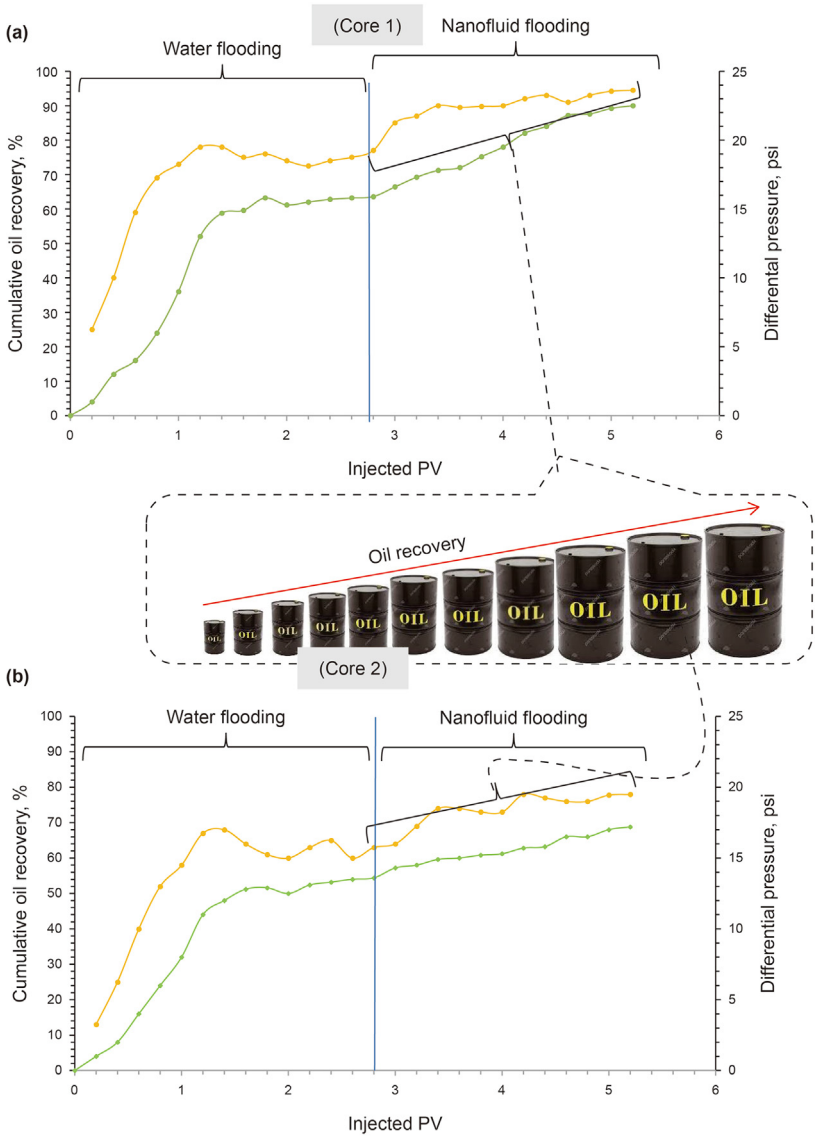

Fig. 17. Cumulative oil recovery and differential pressure in the process of water and synthesized GO-Su-HMDS nanofluid flooding at prepared concentrations of (**a**) 400 and (**b**) 500 ppm.

of the existing rock. In this regard, Fig. 16 shows the possible mechanism of adsorption of GO-Su-HMDS NPs on the surface of carbonate rock.

3.5. Coreflood experiments

In order to evaluate the performance of GO-Su-HMDS NF in the process of injection into the core, the first two concentrations of 400 and 500 ppm for GO-Su-HMDS NF were prepared. Subsequently, a flooding test was performed using this synthesized NF in order to enhance oil recovery. To observe the amount of produced oil, DI water and NF were injected after the core was saturated with crude oil. Fig. 17 shows the curves of the cumulative oil recovery versus the pore volume (PV) injection at different NP concentrations in the core flooding experiments. The breakthrough phenomenon in the flooding process with DI water for the first and second carbonate core plugs was 78% and 63%, respectively. According to the output results of Fig. 17a and b, the share of this NF for the first and second carbonate core plugs in the EOR process was 16.5% and 15%, respectively. Therefore, the ratios of oil recovery through the flooding process in the first and second carbonate core plugs by this NF to the total oil recovery are 20% and 19%, respectively. The calculated values of oil recovery ratio after water and GO-Su-HMDS flooding to overall oil recovery was 94.5% and 78%, respectively. Therefore, these calculated values, in a way, indicate the effective efficiency of this new nanoparticle in the EOR process. According to the given interpretations, it can be concluded that this new nanoparticle has an effective efficiency in moving the oil molecules from the surface of the above oil wet carbonate rock. On the other hand, the differential pressure decreased in the two carbonate core samples, which indicates that there is no significant and beneficial effect of increasing the viscosity in the NF flooding process in the core plugs. Moreover, in the NF injection process, the effect of secondary differential pressure is not as significant as in other mechanisms in EOR. As a result, these curves show that other mechanisms have active impacts on the EOR process.

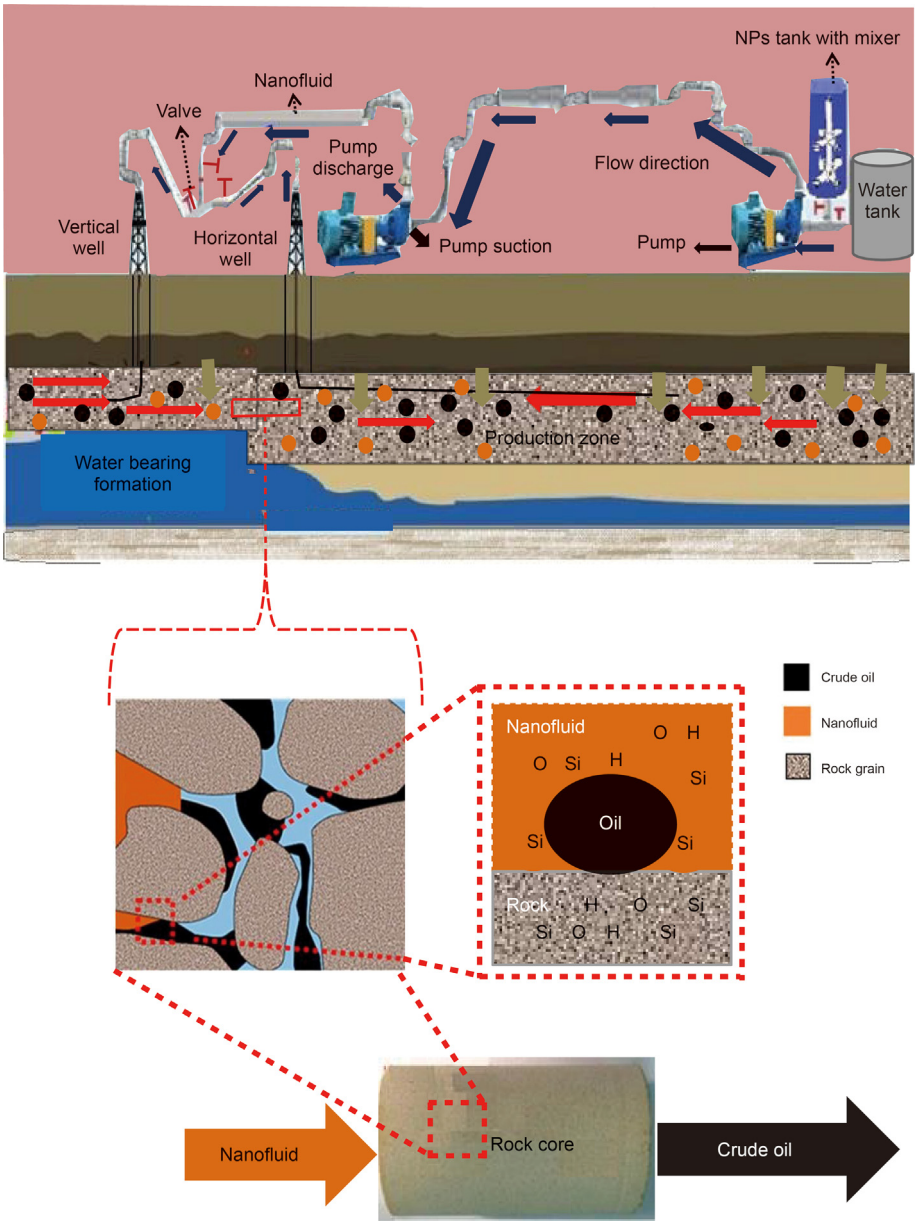

Fig. 18. Illustration representation of nanofluid injection method for future application.

3.6. *Possible mechanisms for the proposed nanoparticle enhanced oil recovery (NP-EOR) technique*

In this study, GO-Su-HMDS nanofluid has advanced in the carbonate porous media. And due to the coordinated structure between the compounds of rock and the compounds of the synthesized NPs, these nanofluids allow some GO-Su-HMDS NPs to be adsorbed on the carbonate rock surfaces and change the rock wettability from oil wet to water wet. On the other hand, some GO-Su-HMDS NPs somehow reduce IFT by being absorbed in the oil-water interface. According to the interpretations presented, the wettability alteration has a significant and efficient role in the mechanism of oil movement from the rock surface. According to the model proposed by Wasan and Nikolov (2003), nanofluids tend to form a wedge film in the contact line of crude oil, nanofluid, and rock phases by adsorption on the rock surface (Cocuzza et al., 2012; Bagherpour et al., 2019; Eltoum et al., 2021), which causes to separate the oil from the rock surface. The mechanism of this wedge film is such that the GO-Su-HMDS nanofluid is placed on the water-oil surface and causes the nanofluid to spread under the oil droplet, thus separating the oil droplet. The mechanism of separation and displacement from the surface is also due to the interaction between the silicon (Si), oxygen (O), hydrogen (H) groups in the synthesized nanoparticle structure with the hydrogen (H), oxygen (O), silicon (-Si) in the surface of the rock surface. In particular, the presence of HMDS functional compounds in the structure of this synthesized nanoparticle has caused the carbonate rock surface to alter from oil wet to water wet state. The mechanism of the nanofluid GO-Su-HMDS is shown schematically in Fig. 18. The red and brown arrows in the pay zone represent horizontal and vertical

sweep efficiency indicating hydrocarbon flow, while orange dots and green spheres represent hydrocarbon and NPs.

4. Conclusions

In this experimental work, various usual EOR experiments were performed to prove the expectation of a successful application of GO-Su-HMDS nanomaterials in the EOR process. The major conclusions are listed as follows:

(1) GO was synthesized using Hummer's method and, then, was subjected to surface modification using sulfonic (S) groups and HMDS. Hence, the presence of silicon (Si) and sulfonic (S) groups in the GO-Su-HMDS structure was confirmed by FT-IR spectra.
(2) At pH values of 3, 6 and 9, the ζ-potential of GO-Su-HMDS NPs was in the proximity of −30 mV, indicating their stable colloidal suspension.
(3) The average droplet size of emulsions decreased from 3.50 to 1.17 μm when increasing the GO-Su-HMDS concentration from 200 to 500 ppm.
(4) Due to the presence of 500 ppm of GO-Su-HMDS NF, IFT between the oil droplet and the water phase decreased from 18.45 to 8.8 mN/m.
(5) The GO-Su-HMDS compounds could be adsorbed on the carbonate surface due to the interaction between the functional compounds and the sheets of the NPs GO-Su-HMDS with the groups in the carbonate rock. The absorption of GO-Su-HMDS NPs on the core at the oil/water/rock contact line indicated that the wettability of the carbonate rock altered by GO-Su-HMDS NPs from oil wet to water wet.
(6) This nanofluid of a concentration of 500 ppm caused the greatest changes in IFT and CA.
(7) The flooding experiments showed that by increasing the nanoparticle concentration from 400 to 500 ppm, the oil recovery was increased by 20% and 19%, respectively.

References

Abbasabadi, M.K., Rashidi, A.M., Khodabakhshi, S., 2016. Benzenesulfonic acid-grafted graphene as a new and green nanoadsorbent in hydrogen sulfide removal. J. Nat. Gas. Sci. Eng. 28, 87–94. https://doi.org/10.1016/j.jngse.2015.11.043.

Abhishek, R., Hamouda, A.A., Ayoub, A., 2018. Effect of silica nanoparticles on fluid/rock interactions during low salinity water flooding of chalk reservoirs. Appl. Sci. 8 (7), 1093. https://doi.org/10.3390/app8071093.

Abu-Al-Saud, M.O., Esmaeilzadeh, S., Riaz, A., Tchelepi, H.A., 2020. Pore-scale study of water salinity effect on thin-film stability for a moving oil droplet. J. Colloid Interface Sci. 569, 366–377. https://doi.org/10.1016/j.jcis.2020.02.044.

AfzaliTabar, M., Alaei, M., Bazmi, M., Ranjineh-Khojasteh, R., Koolivand-Salooki, M., Motiee, F., Rashidi M., A., 2017. Facile and economical preparation method of nanoporous graphene/silica nanohybrid and evaluation of its Pickering emulsion properties for chemical EOR. Fuel 206 (15), 453–466. https://doi.org/10.1016/j.fuel.2017.05.102.

Ahmadi, M.A., Shadizadeh, S.R., 2013. Experimental investigation of adsorption of a new nonionic surfactant on carbonate minerals. Fuel 104, 462–467. https://doi.org/10.1016/j.petlm.2015.11.003.

Ahmadi, S., Hosseini, M., Tangestani, E., Mousavi, S.E., Niazi, M., 2020. Wettability alteration and oil recovery by spontaneous imbibition of smart water and surfactants into carbonates. Pet Sci 17, 712–721. https://doi.org/10.1007/s12182-019-00412-1.

Al-Anssari, S., Barifcani, A., Wang, S., Maxim, L., Iglauer, S., 2016. Wettability alteration of oil-wet carbonate by silica nanofluid. J. Colloid. Interface. Sci. 461, 435–442. https://doi.org/10.1016/j.jcis.2015.09.051.

Alizadeh-Pahlavan, A., Cueto-Felgueroso, L., Hosoi, A.E., McKinley, G.H., Juanes, R., 2018. Thin films in partial wetting: stability, dewetting and coarsening. J Fluid Mech 845, 642–681. https://doi.org/10.1017/jfm.2018.255.

Allan, J., Sun, S., 2003. Controls on recovery factor in fractured reservoirs: lessons learned from 100 fractured fields. In: SPE Annual Technical Conference and Exhibitions. https://doi.org/10.2118/84590-MS.

Alomair, O.A., Matar, K.M., Alsaeed, Y.H., 2014. Nanofluides application for heavy oil recovery. In: SPE Asia Pacific Oil & Gas Conference and Exhibition. https://doi.org/10.2118/171539-MS.

Anderson, W.G., 1986a. Wettability literature survey-part 1: rock/oil/brine interactions and the effects of core handling on wettability. J. Petro. Tech. 38, 1125–1144. https://doi.org/10.2118/13932-PA.

Anderson, W.G., 1986b. Wettability literature survey-part 3: The effects of wettability on the electrical properties of porous media. J. Petro. Tech. 38, 12. https://doi.org/10.2118/13934-PA.

Ayirala, S., Li, Z., Mariath, R., AlSofi, A., Xu, Z., Yousef, A., 2020. Microscale interactions of surfactant and polymer chemicals at crude oil/water interface for enhanced oil recovery. Society of Petroleum Engineers 25 (4), 1812–1826. https://doi.org/10.2118/198574-PA.

Bagherpour, S., Rashidi, A.M., Mousavi, S., Izadi, N., Hamidpour, E., 2019. Experimental investigation of carboxylate-alumoxane nanoparticles for the enhanced oil recovery performance. Colloids. Surf. A Physicochem. Eng. Asp. 563, 37–49. https://doi.org/10.1016/j.colsurfa.2018.11.068.

Belyaeva, L.A., Schneider, G.F., 2020. Wettability of graphene. Surf. Sci. Rep. 100–482. https://doi.org/10.1016/j.surfrep.2020.100482.

Bhuiyan, M.H.U., Saidur, R., Amalina, M.A., Mostafizur, R.M., Islam, A., 2015. Effect of nanoparticles concentration and their sizes on surface tension of nanofluids. Procedia Engineering 105, 431–437. https://doi.org/10.1016/j.proeng.2015.05.030.

Cheng, Y., Zhao, M., Zheng, C., Guo, S., Li, X., Zhang, Z., 2017. Water-dispersible reactive nanosilica and poly(2-acrylamido-2- methyl-1-propanesulfonic acid sodium) nanohybrid as potential oil displacement agent for enhanced oil recovery. Energy & Fuels 31 (6), 6345–6351. https://doi.org/10.1021/acs.energyfuels.7b00743.

Cheraghian, G., Hendraningrat, L., 2016. A review on applications of nanotechnology in the enhanced oil recovery part A: effects of nanoparticles on interfacial tension. Int Nano Lett 6, 129–138. https://doi.org/10.1007/s40089-015-0173-4.

Cocuzza, M., Pirri, C., Rocca, V., Verga, F., 2012. Current and future nanotech application in the oil industry. American Journal of Applied Sciences 9 (6). https://doi.org/10.1021/acs.energyfuels.7b00743, 784-779.

Das, S.K., Choi, S.U.S., Yu, W., Pradeep, T., 2007. Nanofluids: Science and Technology. John Wiley & Sons, Inc., Hoboken, New Jersey https://doi.org/10.1002/9780470180693.

Das, S., Katiyar, A., Rohilla, N., Bonnecaze, R.T., Nguyen, Q.A., 2021. Methodology for chemical formulation for wettability alteration induced water imbibition in carbonate reservoirs. J Petrol Sci Eng 198, 108136. https://doi.org/10.1016/j.petrol.2020.108136.

Dehghan-Monfared, A., Ghazanfari, M.H., Jamialahmadi, M.M., Helalizadeh, A., 2015. Adsorption of silica nanoparticles onto calcite: equilibrium, kinetic, thermodynamic and DLVO analysis. Chem. Eng. J. 281, 334–344. https://doi.org/10.1016/j.cej.2015.06.104.

Eltoum, H., Yang, Y.L., Hou, J.R., 2021. The effect of nanoparticles on reservoir wettability alteration: a critical review. Pet Sci 18, 136–153. https://doi.org/10.1007/s12182-020-00496-0.

Esmaeilzadeh, S., Qin, Z., Riaz, A., Tchelepi, H.A., 2020. Wettability and capillary effects: dynamics of pinch-off in unconstricted straight capillary tubes. Physical Review E 102 (2), 023109. https://doi.org/10.1103/PhysRevE.102.023109.

Fenter, P., Qin, T., Lee, S.S., AlOtaibi, M.B., Ayirala, S., Yousef, A.A., 2020. Molecular-scale origins of wettability at petroleum–brine–carbonate interfaces. Cientific Reports 10. https://doi.org/10.1038/s41598-020-77393-4, 20507.

Fletcher, A., Davis, J., 2010. How EOR can be transformed by nanotechnology. In: SPE Improved Oil Recovery Symposium. https://doi.org/10.2118/129531-MS.

Ghasemi, M., Suicmez, V.S., Sigalas, L., Olsen, D., 2020. Impact of rock properties and wettability on Tertiary-CO2 flooding in a fractured composite chalk reservoir. J. Nat. Gas. Sci. Eng. 77, 103167. https://doi.org/10.1016/j.jngse.2020.103167.

Giraldo, J., Benjumea, P., Lopera, S., Cortes, F., Ruiz, M., 2013. Wettability alteration of sandstone cores by alumina-based nanofluids. Energy & Fuels 27, 3659–3665. https://doi.org/10.1021/ef4002956.

Gomari, S.R., Omar, Y.G.D., Amrouche, F., Islam, M., Xu, D., 2019. New insights into application of nanoparticles for water-based enhanced oil recovery in carbonate reservoirs. Colloids. Surf. A Physicochem. Eng. Asp. 568, 164–172. https://doi.org/10.1016/j.colsurfa.2019.01.037.

Guo, H., Nazari, N., Esmaeilzadeh, S., Kovscek, A.R., 2020. A critical review of the role of thin liquid films for modified salinity brine recovery processes. Curr Opin Colloid Interface Sci 50, 101393. https://doi.org/10.1016/j.cocis.2020.101393.

Hamouda, A.A., Abhishe, R., 2019. Effect of salinity on silica nanoparticle adsorption kinetics and mechanisms for fluid/rock interaction with calcite. Nanomaterials 9 (2), 213. https://doi.org/10.3390/nano9020213.

Hamouda, A.A., Murzin, I., 2019. Influence of individual ions on silica nanoparticles interaction with berea sandstone minerals. Nanomaterials 9 (9), 1267. https://doi.org/10.3390/nano9091267.

Hendraningrat, L., Torsæter, O., 2016. A study of water chemistry extends the benefits of using silica-based nanoparticles on enhanced oil recovery. Applied Nanoscience 6, 83–95. https://doi.org/10.1007/s13204-015-0411-0.

Hendraningrat, L., Li, S., Torsaeter, O., 2013. Effect of some parameters influencing enhanced oil recovery process using silica nanoparticles: an experimental investigation. In: SPE Reservoir Characterization and Simulationn Conference and Exhibition. 10.2118/165955-MS. https://doi.org/10.2118/165955-MS.

Jafarbeigi, E., Kamari, E., Salimi, F., Mohammadidoust, A., 2020. Experimental study of the effects of a novel nanoparticle on enhanced oil recovery in carbonate porous media. J Petrol Sci Eng 195, 107602. https://doi.org/10.1016/j.petrol.2020.107602.

Ji, J., Zhang, G., Chen, H., Wang, S., Zhang, G., Zhang, F., Fan, X., 2011. Sulfonated graphene as water-tolerant solid acid catalyst. Chem. Sci. 2, 484–487. https://

doi.org/10.1039/C0SC00484G.
Kumar, R., Sharma, T., 2018. Stability and rheological properties of nanofluids stabilized by SiO_2 nanoparticles and SiO_2-TiO_2 nanocomposites for oilfield applications. Colloids. Surf. A Physicochem. Eng. Asp. 539, 171–183. https://doi.org/10.1016/j.colsurfa.2017.12.028.
Li, S.J., He, J.Z., Zhang, M.J., Zhang, R.X., Lv, X.L., Li, S., Pang, H., 2013. Electrochemical detection of dopamine using water-soluble sulfonated graphene. Electrochim. Acta. 102, 58–65. https://doi.org/10.1016/j.electacta.2013.03.176.
Mahani, H., Keya, A., Berg, S., Bartels, W.B., Nasralla, R., Rossen, W., 2015. Insights into the mechanism of wettability alteration by low salinity waterflooding (LSF) in carbonates. Energy & Fuels 29 (3), 1352–1367. https://doi.org/10.1021/ef5023847.
Mahani, H., Keya, A.L., Berg, S., Nasralla, R., 2017. Electrokinetics of carbonate/brine interface in low-salinity waterflooding: effect of brine salinity, composition, rock type, and pH on ζ-potential and a surface-complexation model. Society of Petroleum Engineers 22 (1), 53–68. https://doi.org/10.2118/181745-PA.
Marcano, D.C., Kosynkin, D.V., Berlin, J.M., Sinitskii, A., Sun, Z., Slesarev, A., Alemany, L.B., Lu, W., Tour, J.M., 2010. Improved synthesis of graphene oxide. ACS Nano 4 (8), 4806–4814. https://doi.org/10.1021/nn1006368.
Mensah, A.E., Opeyemi, A., Shaibu, M., 2013. Effects of nano particles (Al, Al_2O_3, Cu, CuO) in emulsion treatment and separation. In: SPE Nigeria Annual International Conference and Exhibition. https://doi.org/10.2118/167508-MS.
Mondragon, R., Julia, J.E., Barba, A., Jarque, J.C., 2012. Characterization of silica–water nanofluids dispersed with an ultrasound probe: a study of their physical properties and stability. Powder Technol. 224, 138–146. https://doi.org/10.1016/j.powtec.2012.02.043.
Nowrouzi, I., Mohammadi, A.H., Khaksar-Manshad, A., 2020a. Effects of methanol and acetone as mutual solvents on wettability alteration of carbonate reservoir rock and imbibition of carbonated seawater. J Petrol Sci Eng 195, 107609. https://doi.org/10.1016/j.petrol.2020.107609.
Nowrouzi, I., Mohammadi, A.H., Khaksar-Manshad, A., 2020b. Effect of a synthesized anionic fluorinated surfactant on wettability alteration for chemical treatment of near-wellbore zone in carbonate gas condensate reservoirs. Pet Sci 17, 1655–1668. https://doi.org/10.1007/s12182-020-00446-w.
Peng, C., Xiong, Y., Liu, Z., Zhang, F., Ou, E., Qian, J., Xiong, Y., Xu, W., 2013. Bulk functionalization of graphene using diazonium compounds and amide reaction. Appl. Surf. Sci. 280, 914–919. https://doi.org/10.1016/j.apsusc.2013.05.094.
Qi, L., Song, C., Wang, T., Li, Q., Hirasaki, G.J., Verduzco, R., 2018. Polymer-coated nanoparticles for reversible emulsification and recovery of heavy oil. Langmuir 34, 6522–6528. https://doi.org/10.1021/acs.langmuir.8b00655.
Radnia, H., Solaimany-Nazar, A.R., Rashidi, A.M., 2017. Experimental assessment of graphene oxide adsorption onto sandstone reservoir rocks through response surface methodology. J. Taivan. Inst. Chem. E. 80, 34–45. https://doi.org/10.1016/j.jtice.2017.07.033.
Radnia, H., Rashidi, A.M., Solaimany-Nazar, A.R., Eskandari, M.M., Jalilian, M., 2018. A novel nano-fluid based on sulfonated graphene for enhanced oil recovery. J. Mol. Liq. 271, 795–806. https://doi.org/10.1016/j.molliq.2018.09.070.
Ranka, M., Brown, P., Hatton, T., 2015. Responsive stabilization of nanoparticles for extreme salinity and high-temperature reservoir applications. Adv. Mater. Interf. 7, 19651–19658. https://doi.org/10.1021/acsami.5b04200.
Rezaei-Namin, A., Rashidi, A.M., Gharesheikhlou, A.A., Ghasemy, E., Jalilian, M., 2019. Experimental application of functionalized N-doped graphene for improving enhanced oil recovery. Colloids. Surf. A. Physicochem. Eng. Asp. 581, 123–801. https://doi.org/10.1016/j.colsurfa.2019.123801.
Rostami, P., Sharifi, M., Aminshahidy, B., Fahimpour, J., 2019. Enhanced oil recovery using silica nanoparticles in the presence of salts for wettability alteration. J. Dispersion Sci. Technol. 41 (3), 402–413. https://doi.org/10.1080/01932691.2019.1583575.
Roustaei, A., Saffarzadeh, S., Mohammadi, M., 2013. An evaluation of modified silica nanoparticles efficiency in enhancing oil recovery of light and intermediate oil reservoirs. Egypt. J. Pet. 22, 427–433. https://doi.org/10.1016/j.ejpe.2013.06.010.
Saeb, A., Hosseini, M., Tangestani, E., Mousavi, S.E., Niazi, M., 2020. Wettability alteration and oil recovery by spontaneous imbibition of smart water and surfactants into carbonates. Pet Sci 17, 712–721. https://doi.org/10.1007/s12182-019-00412-1.
Saleh, T.A., AL-Hammadi, S.A., 2018. Insights into the fundamentals and principles of the oil and gas industry: the impact of nanotechnology. Nanotechnology in Oil and Gas Industries 1–35. https://doi.org/10.1007/978-3-319-60630-9_1.
Schramm, L.L., 1992. Emulsions: Fundamentals and Applications in the Petroleum Industry. American Chemical Society, Washington. https://doi.org/10.1021/ef950077m.
Shakiba, M., Khamehchi, E., Fahimifar, A., Dabir, B., 2020. A mechanistic study of smart water injection in the presence of nanoparticles for sand production control in unconsolidated sandstone reservoirs. J. Mol. Liq. 319, 114210. https://doi.org/10.1016/j.molliq.2020.114210.
Suleimanov, B.A., Ismailov, F.S., Veliyev, E.F., 2011. Nanofluid for enhanced oil recovery. J Petrol Sci Eng 78 (2), 31–437. https://doi.org/10.1016/j.petrol.2011.06.014.
Sun, X., Zhang, Y., Chen, G., Gai, Z., 2017. Application of nanoparticles in enhanced oil recovery: a critical review of recent progress. Energies 10, 1–33. https://doi.org/10.3390/en10030345.
Taleb, M., Sagala, F., Hethnawi, A., Nassar, N.N., 2021. Enhanced oil recovery from austin chalk carbonate reservoirs using faujasite-based nanoparticles combined with low-salinity water flooding. Energy & Fuels 35 (1), 213–225. https://doi.org/10.1021/acs.energyfuels.0c02324.
Taylor, R., Coulombe, S., Otanicar, T., Phelan, P., Gunawan, A., Lv, W., Rosengarten, G., Prasher, R., Tyagi, H., 2013. Small particles, big impacts: a review of the diverse applications of nanofluids. J. Appl. Phys. 113 (1), 11–301. https://doi.org/10.1063/1.4754271.
Ture, S., Darcan, C., Türkyılmaz, O., Kaygusuz, O., 2020. Synthesis, structural characterization and antimicrobial activities of cyclochlorotriphosphazene derivatives derived from N-(1-naphthyl)ethylenediamine. Phosphorus, Sulfur Silicon Relat. Elem. 195 (6), 507–515. https://doi.org/10.1080/10426507.2020.1723096.
Tuteja, S.K., Kukkar, M., Suri, C., Paul, A., Deep, A., 2015. One step in-situ synthesis of amine functionalized graphene for immunosensing of cardiac marker cTnI. Biosens Bioelectron 66, 129–135. https://doi.org/10.1016/j.bios.2014.10.072.
Wasan, D., Nikolov, A.D., 2003. Spreading of nanofluids on solids. Nature 423, 156–159. https://doi.org/10.1038/nature01591.
Wei, Y., Babadagli, T., 2018. Changing interfacial tension and wettability using new generation chemicals and nano metal particles at elevated temperatures and pressures: an analysis through a new experimental design for heavy-oil recovery applications. J. Dispersion Sci. Technol. 40 (12), 1785–1794. https://doi.org/10.1080/01932691.2018.1542311.
Yao, Y., Wei, M., Kang, W., 2021. A review of wettability alteration using surfactants in carbonate reservoirs. Adv Colloid Interface Sci 294, 102477. https://doi.org/10.1021/acs.energyfuels.9b03409.
Yao, Y., Mingzhen, W., Baojun, B., 2022. Descriptive statistical analysis of experimental data for wettability alteration with surfactants in carbonate reservoirs. Fuel 310, 122110. https://doi.org/10.1016/j.fuel.2021.122110.
Yin, T., Yang, Z., Dong, Z., Lin, M., Zhang, J., 2019. Physicochemical properties and potential applications of silica-based amphiphilic Janus nanosheets for enhanced oil recovery. Fuel 237, 344–351. https://doi.org/10.1021/acs.iecr.6b03299.
Zhang, H., Ramakrishnan, T.S., Nikolov, A., Wasan, D., 2016. Enhanced oil recovery driven by nanofilm structural disjoining pressure: fooding experiments and microvisualization. Energy & Fuels 2771–2779. https://doi.org/10.1021/acs.energyfuels.6b00035.
Zheng, C., Cheng, Y., Wei, Q., Li, X., Zhang, Z., 2017. Suspension of surface-modified nano-SiO_2 in partially hydrolyzed aqueous solution of polyacrylamide for enhanced oil recovery. Colloids. Surf A Physicochem. Eng. Asp. 524, 169–177. https://doi.org/10.1016/j.colsurfa.2017.04.026.
Zhu, Y., Murali, S., Cai, W., Li, X., Suk, J.W., Potts, J.R., Ruoff, R.S., 2010. Graphene and graphene oxide: synthesis, properties, and applications. Adv. Mater. 22 (35), 3906–3924. https://doi.org/10.1002/adma.201001068.